Fuel-Optimally Guided Navigation and Tracking Control of AUV under Current Interaction

Kangsoo Kim[1] and Tamaki Ura[2]

[1]Graduate School of Engineering, The University of Tokyo
4-6-1 Komaba, Meguro, Tokyo 153-8505, Japan
kskim@iis.u-tokyo.ac.jp

[2]Institute of Industrial Science, The University of Tokyo
4-6-1 Komaba, Meguro, Tokyo 153-8505, Japan
ura@iis.u-tokyo.ac.jp

***Abstract* - Fuel-optimally guided navigation and tracking control of AUV under current interaction is presented. Existence of sea current should be one of the most important considerations for the navigation of AUV, since the speed of it is set low to reduce the fuel consumption as possible. This is because the replenishment during the mission is not possible for AUV, as it attains more motion freedom at the expense of umbilical cable. When an AUV is subjected to transfer between two pre-designated points in the region of sea current, ingenious guidance enables the AUV to reach the terminal position minimizing the fuel consumption. In this paper, fuel-optimal guidance law is derived and applied to the navigation of "R2D4", a newly developed AUV by IIS, the university of Tokyo. Optimal guidance law is formulated as a two-point boundary value problem on the basis of Euler-Lagrange equations. In this formulation, position vector relative to inertial frame is qualified as the state vector, while the vehicle's heading as the input. Simulations of optimal guidance of R2D4 in arbitrarily defined current distributions show as the current distribution becomes more complicated and diverse, gains by optimal guidance become more apparent.**

I. INTRODUCTION

As the last potential supplier of natural resources and energies as well as provisions on the earth, the ocean is requested more and more to reveal its substances to human beings. In order to sustain the ocean development, AUVs (Autonomous Underwater Vehicles) are expected to become one of the most promising means for undersea exploration or exploitation, since the risks on human life are fundamentally got rid of even if there happens serious trouble or failure during the mission. Near the sea surface, wave becomes the major external disturbance that excites any floating body. As the depth of submergence increases, excitation by surface wave decreases rapidly. But even in the middle of undersea region, there exist another kind of disturbances like sea current. On the navigation of AUV, current should be a serious consideration since in general, speed of AUV is set to be not so high in order to restrain the fuel consumption as minimal. When the magnitude of current velocity reaches nearly the same order of vehicle's one, quite amount of drift is induced on the vehicle motion due to the interaction with current flow. Therefore when the vehicle transfers between two points in the current region, it is quite natural there happen considerable differences in elapsed time and energy consumption among each transition along the different trajectory.

Searching for the optimal path over the region of interest has been one of the most frequently mentioned topics in optimal control research. Aerospace engineers especially have treated numerous problems of optimal trajectory planning in view of particular objectives for spacecraft navigation such as minimum time, minimum fuel consumption or maximum payload and so forth. Tsuchiya and Suzuki [3] derived fuel-optimal navigational trajectory of a spacecraft to reach the target height of 400 (km). System dynamics was described within interplanetary attraction field consists of the earth and spacecraft only. In their work, optimal control problem was converted to that of mathematical programming discretizing the control input in time domain. Crespo and Sun [2] proposed cell mapping method to solve the optimal tracking of a moving target in the vortex field. Application of cell mapping showed another possibility in obtaining numerical solution of optimal tracking control in case the system dynamics is strongly nonlinear.

Minimum-time guidance of a ship in the region of current was treated by Bryson and Ho [1]. The problem was formulated by calculus of variations, and the optimal guidance law was derived as an explicit form of ordinary differential equation. Though this guidance law seems comparatively simple, it is not easy to obtain its numerical solution because not only final time, but also initial heading becomes unknowns in this problem, that is, it consists of a so called two-point boundary value problem.

In this research, authors propose an algorithm, which enables us to detect the correct initial heading utilizing the reference final time obtained from Arbitrary REference Navigation (AREN). It is simple but universally applicable algorithm to the arbitrarily distributed current flow if the detailed profile of it is known a priori. Although the actual current distribution also varies in vertical direction, AREN is designed to work only within the horizontal plane. Navigation by other guidance law such as Proportional Navigation (PN) or trajectory tracking control was also presented in order to be used as a possible reference navigation. By comparing the optimally guided navigation with the ones from other guidance laws, efficacy of optimal guidance under given current distribution is clarified.

0-933957-31-9

II. OPTIMAL GUIDANCE OF AUV IN CURRENT FIELD

A. Definition of The Problem

Consider an AUV traveling through a region of strong currents, which depend on the position. The AUV is obliged to start from initial position at $t=0$, and reach the destination at $t=t_f$, the final time. If the throttle of main engine is set fixed during the overall navigation, fuel consumption rate to compensate the power loss by the drag also remains constant. This means if we neglect the additional energy consumption by the operation of actuators which seems relatively small, total fuel consumption decreases as the vehicle reaches the destination earlier. In other words, minimum-time guidance simultaneously achieves the fuel-optimal navigation provided the constraint of fixed throttle is assumed. Fuel-optimal guidance is important for AUV navigation because like spacecraft, fuel supplement during the mission is practically impossible for AUV.

B. Formulation of Optimal Controller

Two sets of coordinate systems are utilized to treat the problem: inertial (earth-fixed) and body-fixed coordinate systems (Fig. 1). Heading of the vehicle is defined as the angle between two x-axes of each coordinate system. Direction of advance velocity of the vehicle is assumed to coincide with x-axis fixed on the vehicle. Though it is not true rigorously, it can be justified since the sideslip angle is kept sufficiently small in case body shape of the vehicle is sufficiently slender. If $u_c(x, y)$ and $v_c(x, y)$ denote components of current velocity vector in a sea region, resultant velocity of the vehicle relative to inertial frame becomes

$$u = \dot{x} = U_0 cos\psi + u_c(x, y) \qquad (2.1a)$$

$$v = \dot{y} = U_0 sin\psi + v_c(x, y) \qquad (2.1b)$$

where,

u, v : x, y components of the vehicle velocity relative to inertial frame
ψ : heading (yaw angle) of the vehicle
U_0 : advance speed of the vehicle

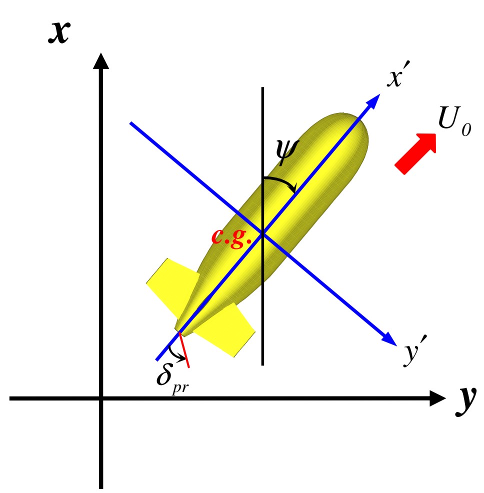

Fig. 1 Inertial and Body-Fixed Coordinate Systems

Let us consider a dynamic model of a system expressed as (2.2), subject to a constraint (2.4) at the final state. A performance index is given as a scalar function of (2.3), which has to be minimized (or maximized) by the optimal control input $u^*(t)$.

Dynamic Model :

$$\dot{\boldsymbol{x}} = \boldsymbol{f}(\boldsymbol{x}, \boldsymbol{u}, t) \qquad (2.2)$$

Performance Index :

$$J = \varphi\{\boldsymbol{x}(t_f), t_f\} + \int_0^{t_f} L(\boldsymbol{x}, \boldsymbol{u}, t)dt \qquad (2.3)$$

Final State Constraint :

$$\boldsymbol{\eta}\{\boldsymbol{x}(t_f), t_f\} = \boldsymbol{0} \qquad (2.4)$$

Controller minimizing the performance index under given constraints can be obtained by solving a set of differential equations, which is so called Euler-Lagrange equations (Bryson and Ho, [1]).

Hamiltonian :

$$H(\boldsymbol{x}, \boldsymbol{u}, t) = L(\boldsymbol{x}, \boldsymbol{u}, t) + \boldsymbol{\lambda}^T \boldsymbol{f}(\boldsymbol{x}, \boldsymbol{u}, t) \qquad (2.5)$$

State Equation :

$$\dot{\boldsymbol{x}} = \frac{\partial H}{\partial \boldsymbol{\lambda}} = \boldsymbol{f} \qquad (2.6)$$

Costate Equation :

$$-\dot{\boldsymbol{\lambda}} = \frac{\partial H}{\partial \boldsymbol{x}} = \left(\frac{\partial \boldsymbol{f}}{\partial \boldsymbol{x}}\right)^T \boldsymbol{\lambda} + \frac{\partial L}{\partial \boldsymbol{x}} \qquad (2.7)$$

Stationary Condition :

$$\boldsymbol{0} = \frac{\partial H}{\partial \boldsymbol{u}} = \frac{\partial L}{\partial \boldsymbol{u}} + \left(\frac{\partial \boldsymbol{f}}{\partial \boldsymbol{u}}\right)^T \boldsymbol{\lambda} \qquad (2.8)$$

Boundary (Transversality) Condition:

$$(\varphi_x + \boldsymbol{\eta}_x^T \boldsymbol{\nu} - \boldsymbol{\lambda})^T\Big|_{t_f} d\boldsymbol{x}(t_f) + (\varphi_t + \boldsymbol{\eta}_t^T \boldsymbol{\nu} + H)\Big|_{t_f} dt_f = 0 \qquad (2.9)$$

where,

t_f	*: final time*
$\boldsymbol{x} \in R^n$, $\boldsymbol{u} \in R^m$	*: state vector / control input vector*
$L(\boldsymbol{x}, \boldsymbol{u}, t)$, $\varphi(\boldsymbol{x}, t)$	*: Lagrangian / final weighting function*
$\boldsymbol{\eta}(\boldsymbol{x}, t) \in R^p$	*: final state function (constraint)*
$\boldsymbol{\lambda} \in R^n$, $\boldsymbol{\nu} \in R^p$	*: Lagrangian multipliers*

Note that dimensions of each vectors represented in (2.2)~(2.9) are $n=2$, $m=1$ and $p=2$ in this problem. For minimum-time control, Lagrangian L in (2.3) should take the value of 1, since the final time t_f becomes the objective to be minimized. Therefore, if we represent the Lagrangian multiplier $\boldsymbol{\lambda}=(\lambda_x\ \lambda_y)$, Hamiltonian is obtainable from (2.1) and (2.5).

$$H = 1 + \lambda_x(U_0 cos\,\psi + u_c) + \lambda_y(U_0 sin\,\psi + v_c) \qquad (2.10)$$

Using the Hamiltonian (2.10), costate equation becomes

$$-\dot{\lambda}_x = \lambda_x \frac{\partial u_c}{\partial x} + \lambda_y \frac{\partial v_c}{\partial x} \quad (2.11a)$$

$$-\dot{\lambda}_y = \lambda_x \frac{\partial u_c}{\partial y} + \lambda_y \frac{\partial v_c}{\partial y} \quad (2.11b)$$

By inserting the Hamiltonian (2.10) into stationary condition (2.8), we can obtain the following relation.

$$tan\,\psi = \lambda_y / \lambda_x \quad (2.12)$$

Terminal position is given and time-invariant, hence $d\boldsymbol{x}(t_f)=0$ in (2.9). If we also consider that the final time is unknown, following condition should be satisfied in (2.9).

$$(\varphi_t + \boldsymbol{\eta}_t{}^T \boldsymbol{\nu} + H)\Big|_{t_f} = 0 \quad (2.13)$$

Since there is no necessary final weighting in this problem, we get

$$\varphi = 0 \quad (2.14)$$

Vehicle has to reach the terminal position at $t=t_f$, so that the final-state constraint may be expressed as

$$\boldsymbol{\eta}(t_f) = \boldsymbol{x}(t_f) - \boldsymbol{x}_{t_f} = \boldsymbol{0} \quad (2.15)$$

From (2.12)~(2.14), we can notice that the final value of the Hamiltonian has to be zero.

$$H(t_f) = 0 \quad (2.16)$$

If we further consider that Hamiltonian for this problem is not an explicit function of time from (2.10), we can obtain

$$\dot{H} = 0 \quad \text{hence} \quad H = const. \quad (2.17)$$

By (2.16) and (2.17), we can conclude that

$$H = 0 \quad \text{for} \quad 0 \le t \le t_f \quad (2.18)$$

By combining (2.10), (2.12) and (2.18), we can solve for λ_x and λ_y:

$$\lambda_x = \frac{-cos\,\psi}{U_0 + u_c cos\,\psi + v_c sin\,\psi} \quad (2.19a)$$

$$\lambda_y = \frac{-sin\,\psi}{U_0 + u_c cos\,\psi + v_c sin\,\psi} \quad (2.19b)$$

Time derivatives of (2.18a,b) become

$$\dot{\lambda}_x = \frac{A\dot{\psi} sin\,\psi + \dot{A} cos\,\psi}{A^2} \quad (2.20a)$$

$$\dot{\lambda}_y = \frac{-A\dot{\psi} cos\,\psi + \dot{A} sin\,\psi}{A^2} \quad (2.20b)$$

where, $A = U_0 + u_c cos\,\psi + v_c sin\,\psi$

Combination of (2.11), (2.19) and (2.20) leads the differential equation for optimal control input $\psi^*(t)$.

$$\dot{\psi} = sin^2\psi \frac{\partial v_c}{\partial x} + \left(\frac{\partial u_c}{\partial x} - \frac{\partial v_c}{\partial y}\right) sin\,\psi cos\,\psi - cos^2\psi \frac{\partial u_c}{\partial y} \quad (2.21)$$

III. METHOD OF NUMERICAL SOLUTION

A. Two-Point Boundary Value Problem

Though it seems not so difficult to obtain the numerical solution of (2.21), there still remains a fatal pitfall. Correct value of the initial heading is still unknown; rather it consists of a part of the solution. This has been predicted difficulty since in Euler-Lagrange equations, values of costates are given at final time while those of states are at initial time. In deriving (2.21), costates are eliminated and made implicit. This causes the appearance of another unknown, the initial heading in (2.21). In fact, Euler-Lagrange equations are one of the typical examples of two-point boundary value problem. To solve the two-point boundary value problem, we have to treat the states and costates simultaneously, relying on an iterative numerical scheme such as shooting or relaxation method. This is quite difficult work of course, requiring the ingenious trial and errors until the solution converges properly.

In this work, instead of direct application of these numerical schemes, we propose a numerical solution procedure that uses the integration of (2.21) on the basis of an iterative searching algorithm that finds out the correct initial heading. Needless to say, it is the simplest and most reliable solution method for our problem, provided the correct initial heading is to be attainable.

B. Utilization of Arbitrary Reference Navigation (AREN)

The simplest way to find out the correct initial heading is to testify the several guesses whether the vehicle's position at $t=t_f$ converges to the desired terminal position. Notice that only the finite number of discrete guesses suffices because the heading is confined within the range of 2π. But we do not know how long we should continue the time integration not to miss the convergence when the guess of $\psi_0^{(i)}$ was the correct one. The present work proposes a methodology to settle this difficulty. If t_f^* denotes the optimal final time, any reference final time t_{f_ref} obtained from arbitrarily guided navigation becomes $t_f^* \le t_{f\_ref}$ by the definition of optimality. When we iteratively carry out the time integration over the range of $0 \le t \le t_{f\_ref}$ changing the guesses of initial heading successively, if a guess has been the correct one vehicle's position must converge to the desired terminal position at $t= t_f^* \le t_{f\_ref}$. If we represent $t_{f\_min}^{(i)}$ as the time when the vehicle approaches the terminal position with minimum deviation of $l_{min}^{(i)}$ during the *i-th* trial navigation started from initial heading guess $\psi_0^{(i)}$, optimal final time t_f^* can be determined by selecting $t_{f\_min}^{(k)}$, which satisfies the relation $l_{min}^{(k)} \le l_{min}^{(j)}$ for any *j-th* trial navigation started from $\psi_0^{(j)}$.

Concept of proposed algorithm is depicted in Figs. 2a,b. As mentioned previously, reference final time t_{f_ref} can be assigned as the elapsed time to reach the terminal position by arbitrarily guided navigation. In this research, elapsed time taken from proportional navigation, which is the simplest navigational law to track a target which moves under relative velocity with the chaser, is used as the reference final time.

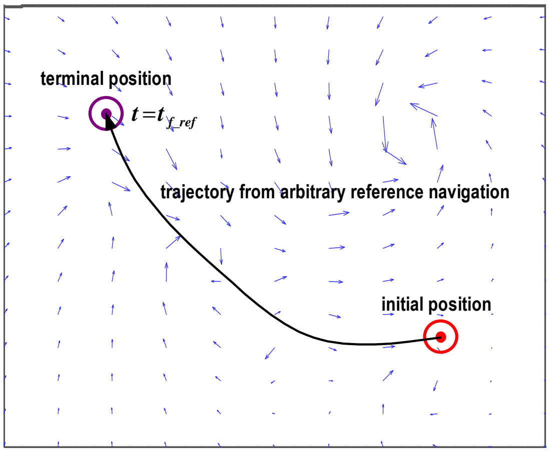

Fig. 2a Determination of the Reference Final Time

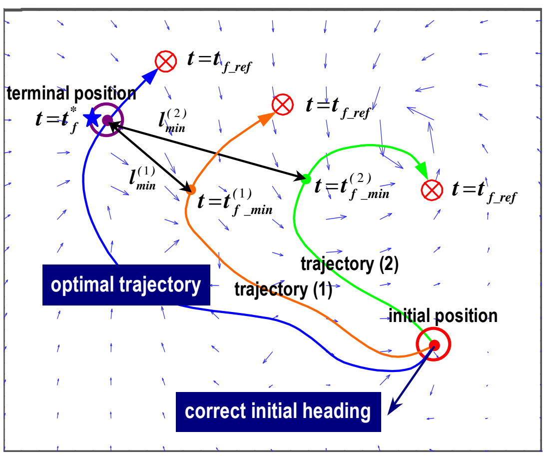

Fig. 2b Detection of the Correct Initial Heading

IV. TRACKING CONTROL SYSTEM DESIGN

A. Motion Control System Design

In this research, a newly developed AUV "R2D4" (Fig. 3) is taken as the plant hardware. R2D4 is a cruising type AUV developed by cooperation between IIS, the university of Tokyo and Mitsui Engineering & Shipbuilding. The most important mission expected for R2D4 is the autonomous survey of undersea thermal vents. In general, undersea thermal vents are located at the bottom of deep sea region, so that the maximum operating depth of R2D4 is designed to reach 4000 (m). Undersea thermal vents are believed to have some significant correlations with the occurrence of earthquakes, which emphasizes the importance of their survey. Principal dimensions with powering specifications of R2D4 are summarized in Table I.

Fig. 3 R2D4 under Construction

Table I Principal Dimensions and Powering Spec. of R2D4

Principal Dimensions		Powering Specifications	
Length Overall (m)	4.0	Designed Speed (m/s)	1.544
Main Body Diameter (m)	0.96	Drag at Designed Speed (N)	128.5
Mass (kg)	1178	Max. Operating Depth (m)	4000

As a part of R2D4 development project, we designed a heading and a depth control system, each of which takes charge of adjusting lateral and longitudinal vehicle motion respectively. At first, we derived a dynamic model of R2D4, which is a basic task to accomplish the control system design. Through the application on the "R-One", the predecessor of R2D4 in IIS, university of Tokyo, we already have established a full CAE based vehicle dynamics modeling procedure, which does not necessitate the scaled model test (Kim and Ura, [4]). By means of this approach, we completed the dynamic models of R2D4, consisting of longitudinal (surge, heave, pitch) and lateral (sway, roll, yaw) coupling modes. As a first step of vehicle dynamics modeling, we carried out CFD analyses in order to obtain the hydrodynamic loads. Fig. 4 shows the pressure distribution with a few traced streamlines, obtained from the CFD analysis of R2D4.

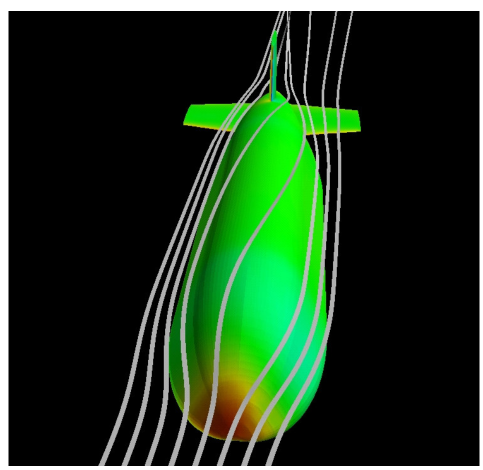

Fig. 4 Pressure Distribution with Streamlines on R2D4

After evaluating all the necessary hydrodynamic loads, stability derivatives are calculated to complete the equations of vehicle motion. When the obtained stability derivatives are placed in the equations of motion, dynamic model of the vehicle is completed. Refer to [4] for the details of CAE based dynamic model construction of AUV.

Results of vehicle motion simulation in horizontal plane are shown in Fig. 5. By solving the equations of motion in time domain with specified actuator input (Fig. 5a, left), motion responses and resulting trajectory are obtained.

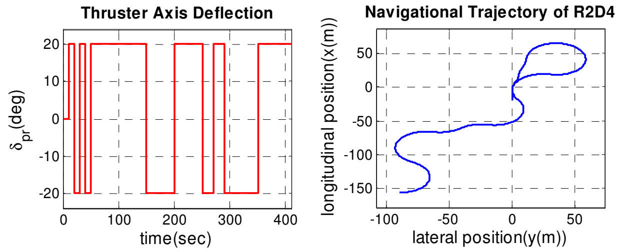

Fig.5a Actuator Input (Left) and corresponding Cruising Trajectory (Right) of R2D4

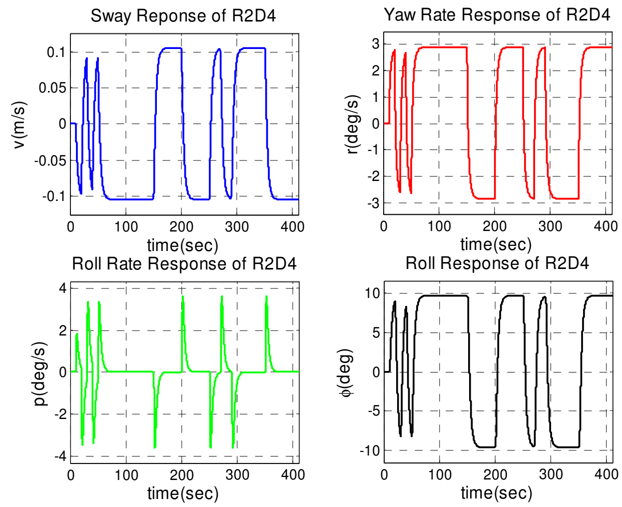

Fig.5b Horizontal Motion Responses of R2D4

Based on the derived dynamic models of R2D4, motion control systems are designed. PID compensations are applied in control system design to ensure the stability and acceptable performances of the compensated closed-loop system. Fig.6 shows the constitution and step response of the designed heading control system.

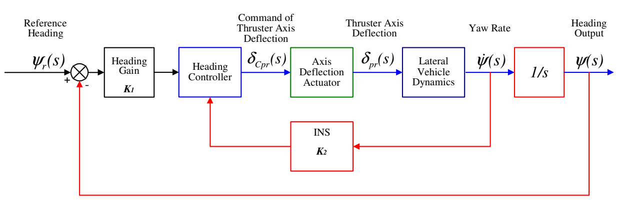

Fig. 6a Block Diagram of Heading Control System for R2D4

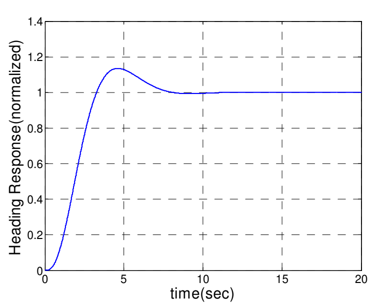

Fig. 6b Step Response of Heading Control System for R2D4

B. Trajectory Tracking Control of AUV under Current

Optimally guided navigation is actually implemented by tracing the target optimal heading series in time domain, obtained as the solution of optimal guidance law explained in section II. Optimal heading tracking is achieved by the action of the heading controller, of course. In this research, not only a heading controller for a mere proportional navigation, but the trajectory tracking controller which makes the vehicle trace the given reference trajectory under current interaction is also developed and designed. The basic idea of the tracking control is quite simple [4]. It modifies the heading command generated by proportional navigation law to cancel out the component of current velocity vector normal to the reference trajectory at present position. This modification leaves only the resultant velocity component tangential to the reference trajectory, which guides the vehicle to slide on it (Fig. 7).

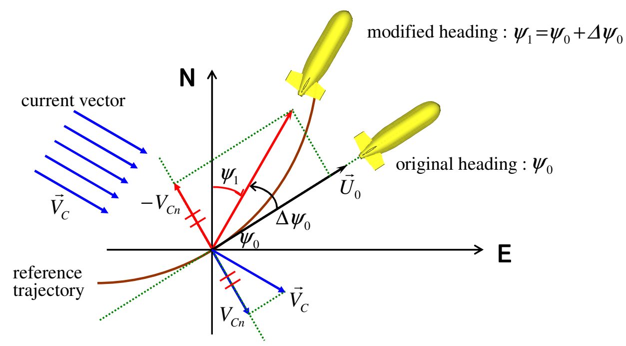

Fig. 7 Concept of Trajectory Tracking Control under Current Interaction

V. RESULTS OF CALCULATION

A. Optimal Guidance in a Shearing Current

If the distribution of current velocity is such that linearly varying profile only in one direction like shearing flow, analytic solution for optimal guidance law is obtainable (Bryson and Ho, [1]). Given the current velocity profile expressed by (5.1a) and (5.1b).

$$u_c(x, y) = 0 \tag{5.1a}$$

$$v_c(x, y) = -U_0(x/h) \tag{5.1b}$$

where,

h : constant proportional coefficient

Equation (5.2a,b) is the analytic optimal guidance law adapting to the current distribution defined as (5.1a,b).

$$\frac{x}{h} = csc\psi - csc\psi_f \tag{5.2a}$$

$$\frac{y}{h} = -\frac{1}{2}\Big[csc\,\psi_f\left(cot\,\psi_f - cot\,\psi\right) - cot\,\psi\left(csc\,\psi_f - csc\,\psi\right) + ln\frac{cot\,\psi_f + csc\,\psi_f}{cot\,\psi + csc\,\psi}\Big] \tag{5.2b}$$

where,

ψ_f : final heading

In order to confirm whether the proposed solution algorithm works properly, numerically simulated optimal guidance under this shearing current is compared with the result by analytic guidance law of (5.2a,b). Proportional navigation guided by simple heading controller is simulated first in order to determine the reference final time t_{f_ref}. By fuel-optimal guidance, vehicle is steered to start from the initial position (x_0, y_0) at $t=0$ and subjected to arrive at the terminal position (x_f, y_f) at $t=t_f$, making the final time t_f converge its minimum value t_f^*. Throttle of the main engine is fixed during the entire navigation, that is, navigation of minimum fuel becomes identical with that of shortest navigation time. During the iterative calculations for trial navigations, guesses of initial heading are set to vary with the increment of 0.5°. Numerical values used in this simulation are summarized in Table II.

Table II
Numerical Data for the Simulation

Initial Position		Terminal Position		Vehicle Speed	Proportional Constant
x_0 (m)	y_0 (m)	x_f (m)	y_f (m)	U_0 (m/s)	h (m)
-186.0	366.0	0.0	0.0	1.544	100.0

As shown in Fig. 8, optimal trajectory obtained from numerical calculation shows no discrepancy with that from analytic solution. Solutions of initial / final heading and navigation time are summarized in Table III.

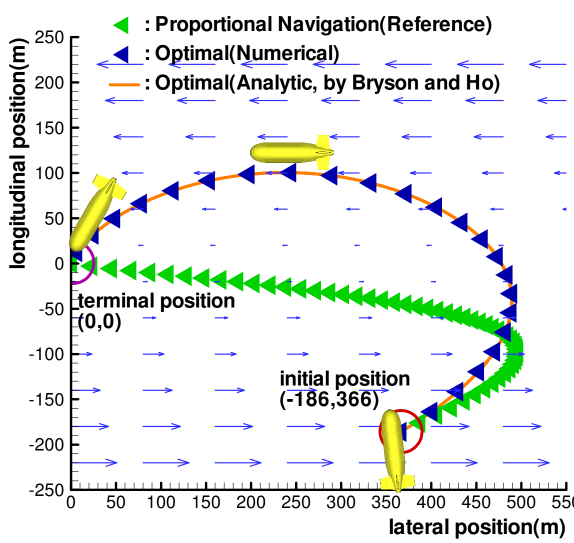

Fig. 8 Optimally Guided Navigation in a Shearing Current

Table III Results of Optimally Guided Navigation in a Shearing Current

	Optimal		PN (Reference)
	Analytic	Numerical	
Initial Heading (deg.)	345	345.0	296.94
Final Heading (deg.)	210	210.1	274.16
Navigation Time (sec)	353.8	353.7	739.17

B. Optimal Guidance in a Current Induced by Two Vortical Sources

One of the most fundamental reasons for sea current may be the ocean circulation owing to the rotation of the earth and global thermal balance. Though globally surveyed mainstream of the ocean circulation is nearly unidirectional, its local profile and distribution changes a lot since there are many other sources of local fluid motion such as tides, thermal convection in vertical plane or flow disturbance by the features of underwater geography. Therefore, it can be imagined that local current velocity distribution in sea area shows more or less complicated profile in its magnitude and direction. Accordingly, except for very few cases as shown in above example, optimal guidance law has to be obtained numerically.

At first, optimal guidance law calculated by the numerical scheme of AREN is testified in the current field generated by two vortical sources. Each vortical source consists of the superposition of a point source (sink) and a vortex, having constant strength (Table IV). In order to prevent from the infinity velocity at the point of location, magnitude of induced flow velocity is restricted to remain under the prescribed upper limit value. Components of current velocity at (x, y) are able to be calculated by (5.3).

$$u_c(x,y) = \frac{m(x - x_{vs}) - K(y - y_{vs})}{r^2} \tag{5.3a}$$

$$v_c(x,y) = \frac{m(y - y_{vs}) + K(x - x_{vs})}{r^2} \tag{5.3b}$$

where,
(x_{vs}, y_{vs}) : position of vortical source
r : distance between vortical source and field point
m : source strength
K : vortex strength

Table IV Properties of Vortical Sources

No.1 Vortical Source			No.2 Vortical Source		
m	K	vel. limit (m/s)	m	K	vel. limit (m/s)
-20	-25	0.8004	-20	20	0.7071

Figs. 9~11 show the navigation trajectories obtained from three (3) different guidances (PN, straight line tracking and optimal) as the distance between two vortical sources varies. Vehicle speed is set to be 1.544(m/s) in these calculations. If there is no current, it is clear that straight line drawn to connect the initial and terminal points becomes the optimal trajectory. In case of uniform flow current having constant velocity all over the region, considering the gradients of the current velocity components become zero, (2.21) gives

$$\dot{\psi} = 0 \quad \text{therefore,} \quad \psi = const. \tag{5.4}$$

From (5.4), we can notice that optimal navigation in the uniform flow current is identical with that of straight line tracking which interconnects the initial and terminal points.

Of course, vehicle cannot trace this straight line by the proportional navigation because of the induced drift by current interaction. Instead, trajectory tracking control as well as optimal guidance may be used to yield the optimal navigation for the uniform current distribution. In Fig. 9a, notice that current distribution around the middle region is near uniform. Therefore, not only the other two trajectories obtained by proportional and trajectory tracking navigations, optimal guidance also yields the trajectory analogous to the straight line as expected. As the two vortical sources get closer, current velocity profile changes more disturbed, which means that the optimal trajectory may appear away from the straight line. In Fig. 9b, optimal guidance makes the vehicle go toward the terminal position detouring the no.2 vortical source. By this detour, vehicle attains the favorable flow components of the current, which prevails over the slightly increased navigation distance. As the two vortical sources get still closer, optimal guidance yields the optimal trajectory appearing on the opposite side, adapting to the given current distribution (Fig. 9c).

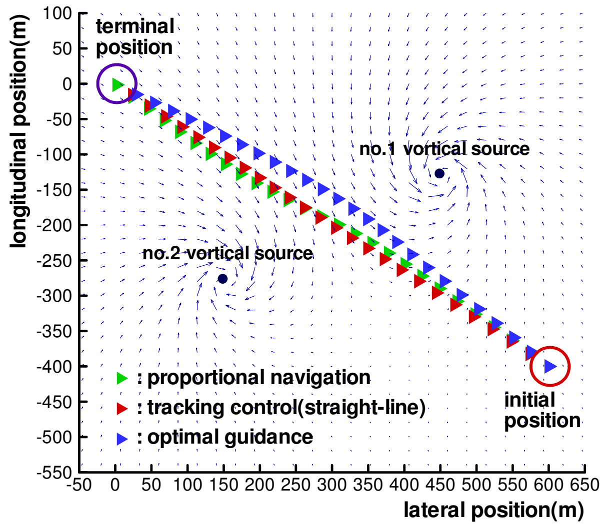

Fig. 9a Navigation Trajectories of R2D4 in a Current Induced by Two Vortical Sources (Case 1 of 3)

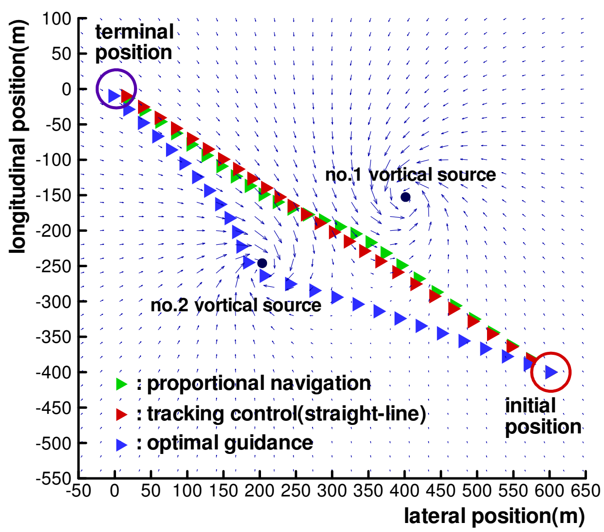

Fig. 9b Navigation Trajectories of R2D4 in a Current Induced by Two Vortical Sources (Case 2 of 3)

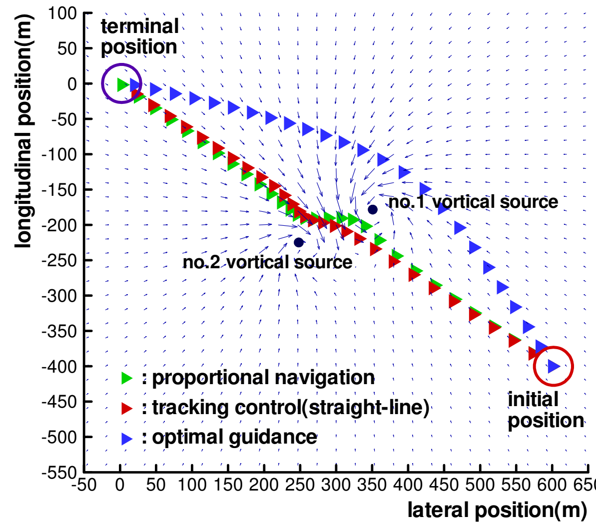

Fig. 9c Navigation Trajectories of R2D4 in a Current Induced by Two Vortical Sources (Case 3 of 3)

Results of navigations in each current distribution induced by two vertical sources are shown in Table V. Notice that effect of optimal guidance is more prominent as the profile of current flow becomes more complicated, mixed with adverse as well as favorable directional flows.

Table V Navigation Results in a Current Induced by Two Vortical Sources

Case No.	Performances	Non-Optimal		Optimal
		PN	Tracking	
Case 1	Elapsed Time (sec)	523.8	518.4	518.2
	Energy Consumption (kJ)	103.9	102.9	102.8
Case 2	Elapsed Time (sec)	534.6	534.6	523.2
	Energy Consumption (kJ)	106.1	106.1	103.8
Case 3	Elapsed Time (sec)	583.2	577.8	493.8
	Energy Consumption (kJ)	115.7	114.6	98.0

C. Optimal Guidance in an Arbitrarily Distributed Current

Next, simulation of the optimal guidance in an arbitrarily distributed current has been attempted. Numerical solution of the optimal guidance law is found by AREN, followed by the optimal heading tracking to implement the optimal navigation. In Fig. 10, while the guidance by proportional navigation or tracking control get much difficulty faced with strong adverse flows near middle region, optimal guidance ingeniously leads the vehicle to go around, so that make use of the favorable current flows. Near the middle region, not only proportional navigation but also tracking control shows much drifted trajectory, having failed in tracing the straight line. This is because the magnitude of current velocity is too large so that the heading modification cannot completely cancel out the trajectory normal component of it.

In this example, distributed profile of the current velocity showing both favorable and adverse directions, as well as large magnitude of it results in large gains in fuel consumption by optimal guidance.

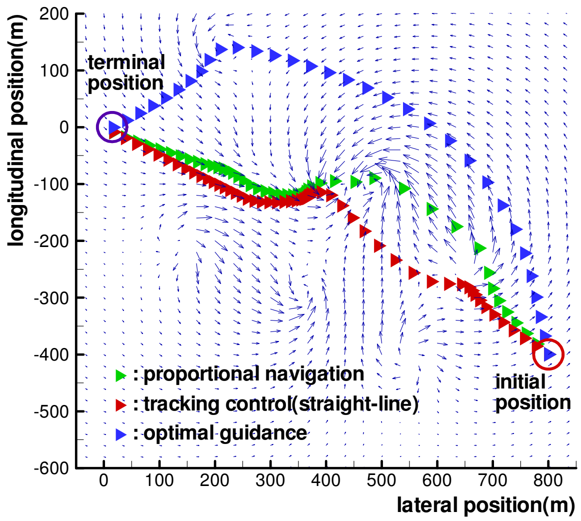

Fig. 10 Navigation Trajectories of R2D4 in an Arbitrarily Distributed Current

Table VI Navigation Results in an Arbitrarily Distributed Current

Performances	Non-Optimal		Optimal
	PN	Tracking	
Elapsed Time (sec)	977.4	1117.8	630.6
Energy Consumption (kJ)	193.9	221.8	125.1

Fig. 11 shows time series of the experienced vehicle headings, generated by three (3) individual guidances.

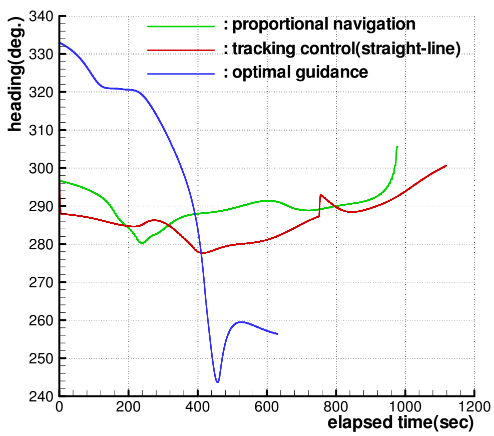

Fig. 11 Time Series of Headings during the Navigations in an Arbitrarily Distributed Current

Once the optimal heading is obtained, it is tracked by a heading controller to complete the optimal navigation. Fig.12 shows the time series of actuator input resulting in the required motion response to achieve the tracking control of optimal heading described in Fig. 11. In case of R2D4, axis of main thruster is designed to be deflectable within horizontal plane, in order to derive the necessary lateral motion responses (sway, yaw and roll). Since the deflectable range is designed to be -20º ~ +20º, actuator input shown in Fig. 12b with its maximum magnitude of 7.3º is able to be executed without any difficulty. Therefore, provided the components of control system work properly, optimally guided navigation is expected to be achieved in actual sea operation, as well as in simulation.

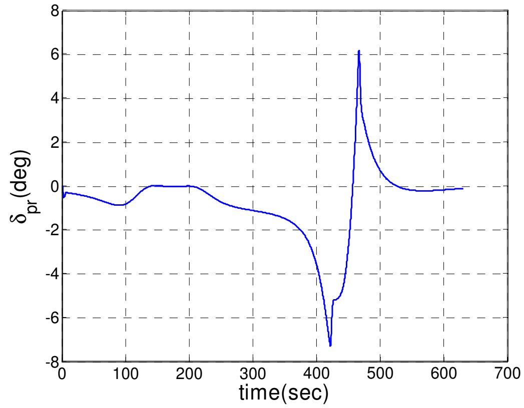

Fig. 12 Time Series of Actuator Input Achieving the Optimal Heading Tracking Control

VI. CONCLUSIONS

Fuel-optimal guidance of AUV under current interaction is presented and analyzed numerically. The problem is formulated by Euler-Lagrange equations and an explicit form of optimal control input is derived as a two-point boundary value problem. To obtain the solution of this problem, a numerical scheme utilizing arbitrary reference navigation named "AREN" is proposed. Optimally guided navigations of AUV "R2D4" in currents induced by two vortical sources show gains by optimal guidance primarily depends on the features of current distribution. Developed scheme has no restriction on the characteristics of current profile, so that it enables the fuel-optimally guided transfer of an AUV if only the distribution of it is known within the sea region of interest.

Acknowledgments

This research is supported by Fundamental Research Developing Association for Shipbuilding and Offshore (REDAS), managed by the Shipbuilder's Association of Japan.

REFERENCES

[1] A.E. Bryson Jr. and Y.C. Ho, "Applied Optimal Control," *Taylor & Francis,* 1975.

[2] L.G. Crespo and J.Q. Sun, "Optimal Control of Target Tracking with State Constraints via Cell Mapping," *J of Guidance, Control, and Dynamics*, Vol 24, No 5, pp 1029-1031, 2001.

[3] T. Tsuchiya and S. Suzuki, "Computational Method of Optimal Control Problem Using Mathematical Programming (1st Report)," *Transactions of Japan Society for Aeronautical and Space Science*, Vol 45, No 519, pp 231-237, 1997.

[4] K. Kim, and T. Ura, "3-Dimensional Trajectory Tracking Control of an AUV "R-One Robot" Considering Current Interaction," *Proc 12th International Offshore and Polar Engineering Conference,* ISOPE-2002, Kita-Kyushu, Vol 2, pp277-283, May 2002.